Pergamon

CEMENT AND CONCRETE RESEARCH

Cement and Concrete Research 29 (1999) 1549–1554

Fundamental study on aluminophosphate cement

Li Shiqun*, Hu Jiashan, Liu Biao, Zhang Guohui, Cao Wei, Wang Qi, Zhang Ning

Department of Materials Science and Engineering, Shandong Building Materials Institute, 250022 Jinan, People's Republic of China

Received 19 March 1998; accepted 26 May 1999

Abstract

Aluminophosphate cement (APC), which contains its own cementitious phases with high hydration performances, has been developed here by a sol-gel process. The main phases of APC synthesized are a new quaternary compound designed according to crystallochemistry principle that is tentatively called "phase S," modified CA ($CaO \cdot Al_2O_3$) and α-C_3P ($3CaO \cdot P_2O_5$), and a certain amount of amorphous phase. The pastes that possess hydration performances of early high strength and increasing long-term strength have been derived from this cement. The analysis of X-ray diffraction, infrared spectra, electronic probe of microarea analysis, and X-ray photoelectron spectroscopy were employed to understand the hydration behavior of APC. © 1999 Elsevier Science Ltd. All rights reserved.

Keywords: Aluminophosphate cement; Hydration performances; Phase composition and structure

1. Introduction

Aluminophosphate cement has been developed in different ways for the last half century. Kingery [1] reviewed the literature on phosphate bonding in refractories up to 1950, and Cassidy [2] summarized the progress that had been made since then regarding the chemistry of the initial bond, alteration of the bond by heat, and applications of phosphate-bonded refractories. Sugama and Carciello [3,4] have reported aluminum phosphate cement formed by the hydrothermal-catalyzed acid-base reaction between alumina and $NH_4H_2PO_4$. A moderate combination of amorphous ammonium aluminum orthophosphate (AmAOP) and crystal $AlPO_4$ in the cement bodies was responsible for the development of strength, but the highest compressive strength cannot reach 10 MPa (100°C), and excess amorphous-to-crystal phase transition resulted in loss in strength. Fang Yonghao et al. [5] have researched the system of phosphate-high alumina cement (HAC) for chemically bonded ceramics (CBC) materials based on the reaction between $(NaPO_3)_n$ and HAC, and have produced high strength pastes. The present paper intends to create a kind of aluminophosphate cement that has its own cementitious phases with high hydration performances.

2. Experimental

2.1. Raw materials

Synthesized cement studied here has been chemically prepared [analysis reagent (AR)]: H_3PO_4, $Ca(NO_3)_2 \cdot 4H_2O$ and $Al(NO_3)_3 \cdot 9H_2O$ and silica sol (industrial, solid content: 26.7% in wt.).

2.2. Chemical and phase composition designing

The compositions of synthesized material are distributed in the calcium-aluminum-rich regions in the subtetrahedron

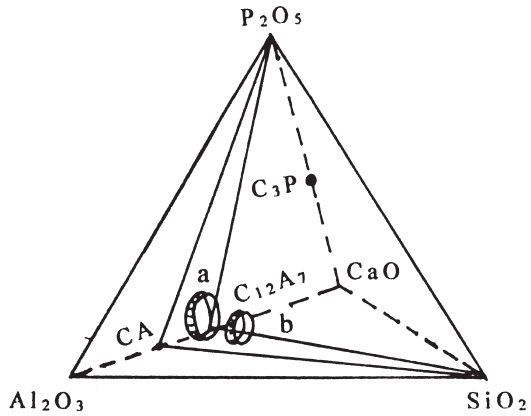

Fig. 1. Distribution of composition designed in quaternary system CaO-Al_2O_3-P_2O_5-SiO_2.

* Corresponding author. Tel.: +86-531-796-3250; fax: +86-531-796-3127.

E-mail address: shiqunli@dns.sdibm.edu.cn (S. Li)

0008-8846/99/$ – see front matter © 1999 Elsevier Science Ltd. All rights reserved.
PII: S0008-8846(99)00111-8

Table 1
Chemical and crystal phase compositon of samples

Region	Sample no.	Basicity*	S**/A + P (in mole)	Crystal phase	Region	Sample no.	Basicity*	S**/A + P (in mole)	Crystal phase
a	012	0.9094	0.1802		b	014	0.7833	0.3077	S
	013	0.7738	0.1627	S, α-C_3P, CA		015	0.7518	0.3002	
	021	0.9007	0.2268			016	0.6566	0.2731	S, α-C3P
	022	0.8139	0.2124			017	0.7168	0.3688	
	023	1.1034	0.0600			018	0.6937	0.3591	
	024	0.9425	0.0545			019	0.6097	0.3271	

*Molar ratio of CaO to the sum of P_2O_5, SiO_2, and Al_2O_3.
**$SiO_2/Al_2O_3 + P_2O_5$.

$CA\text{-}C_{12}A_7\text{-}P_2O_5\text{-}SiO_2$ of the quaternary phase diagram $CaO\text{-}Al_2O_3\text{-}P_2O_5\text{-}SiO_2$, as shown in Fig. 1 and Table 1. Phase composition designing has been dealt with based on crystallochemical principles. Table 2 shows the main crystallochemistry data [6] of the ions concerned here. Tables 3 and 4 list the density variation. It can be seen that the density decreases with respective content of P_2O_5 or SiO_2 increment, while maintaining the mole ratio of other elements constant, if the content of P_2O_5 or SiO_2 is limited in a certain interval as studied in this paper. From the above three tables, it could be inferred that once the ions Al^{3+}, P^{5+}, and Si^{4+} substitute for one another in the network structure of tetrahedron, on the one hand, the lattice would be distorted by the unequal bond force and ionic size; on the other hand, lattice defects would be created for maintaining electrovalency equilibrium, and thus bring an unstable and high activity crystal phase. The possible defect reactions might be as shown in Eq. (1):

$$2SiO_2 \xrightarrow{P_2O_5} 2\,Si_p' + V_0^{\cdot\cdot} + 4O_0$$

$$SiO_2 \xrightarrow{Al_2O_3} Si_{Al}^{\cdot} + V_{Al}''' + V_0^{\cdot\cdot} + 2O_0$$

$$3P_2O_5 \xrightarrow{5A1_2O_3} 6P_{Al}^{\cdot\cdot} + 4V_{Al}''' + 15O_0$$

$$2SiO_2 + P_2O_5 \xrightarrow{3Al_2O_3} 2\,Si_{Al}^{\cdot} + 2\,P_{Al}^{\cdot\cdot} + 2V_{Al}''' + 9O_0 \qquad (1)$$

For the reasons given above, hopefully, a new quaternary compound with good hydration behavior might be created and the modified aluminate and phosphate phases can been expected.

2.3. Synthesis and hydration of aluminophosphate cement

Six compositions have been selected in regions (a) and (b), respectively, in the designed range shown in Table 1. The fabricated gel was preheated at 750°C for 2 h, then at 1550°C for 2 h, and was quenched in air immediately. Next, the material was ground to pass through a no. 325 sieve, and then was molded with 12.5 MPa pressure (water/cement = 0.2) into specimens, size 10 × 10 × 40 mm, and cured for 1, 3, 7, 28, 90, and 180 days in water at 20 ± 2°C. The compressive strength of specimens was tested at the designated age. After that, the hydration of specimens was stopped by alcohol (AR) for the next analysis.

2.4. Measurement procedures and date analysis

Phase analysis for powder samples after sintering was conducted by D/max-ra-II Rigaku X-ray diffractometer (XRD) (Japan) with the experimental condition of voltage/current as 40 kV/80 mA. Infrared spectroscopy analysis (IR) was performed by IR Bio-Rad FTS-165 instrument (USA), and the resolution and accuracy were 0.17 and 0.01 cm^{-1}, respectively. X-ray photoelectron spectroscopy (XPS) measurements were carried out by an XPS (ESCALAB MK II, VG Scientific Ltd., England), which has already been described in some detail in the literature [7]. An Mg K_α 250 W source ($h\nu$ = 3.15 KeV) was used. The spectra were calibrated by utilization of the C_{1S} peaks [binding energy (BE) = 284.6 eV], and the characteristic kinetic energy of the analyzer (CAE) was 50 eV. By subtracting the background and 19 points smooth treatment to get rid of noise, using

Table 2
Crystallochemistry data [6] of ions P^{5+}, Al^{3+}, and Si^{4+}

Species of cation	Ionic radius (nm, CN = 4)	Bond energy M-O (KJ)	Distance of bond M-O (nm)	Volume of $[MO_4]^{n-} \times 10^{-4}$ (nm^3)
P^{5+}	0.017	465–369	0.152	4.3886
Si^{4+}	0.026	444	0.162	5.1983
Al^{3+}	0.039	>330	0.172	6.5351

Table 3
Density variation with P_2O_5 addition in $CaO\text{-}Al_2O_3$ system*

Sample no.	P_2O_5 (in mole)	Density (g/cm^3)
006	0.04931	1.9487
007	0.08454	1.4750
008	0.11976	1.3872
009	0.15498	1.6408

*C_aO/Al_2O_3 = 1.79 (in mole).

Table 4
Denisity variation with SiO_2 in $CaO\text{-}Al_2O_3\text{-}P_2O_5$ system*

Sample no.	SiO_2 (in mole)	Density (g/cm^3)
001	0.02996	2.8712
002	0.09820	2.4722
003	0.10286	2.4384

*$C_aO/Al_2O_3 + P_2O_5 + SiO_2 = 1.40$ (in mole).

two times derivative deconvolution, the energy position and relative intensity of the four chemical states of Ca_{2P} for the original spectrum can be defined (see Fig. 4), then these parameters can be put into the fitting program to derive the fitting curve of the relevant four peak positions. In order to compare the composition of phase S with that synthesized by Zhang [8], the quantitative analysis of electronic probe of microarea analysis (EPMA) with election spectroscopy for chemical analysis (ESCA) was conducted with the Mode JXA-73 instrument (Japan) by the ESCA-Link Company, England (AN10/855; inner standards: GaP for P element, $\alpha\text{-}Al_2O_3$ for Al, wollastonite for Ca; orthoclase for Si, corrective element: Co).

3. Results and discussions

3.1. Phase composition analysis in synthesized APC

Aluminophosphate cement synthesized here is mainly composed of crystalline phases S, CA, and $\alpha\text{-}C_3P$, and a certain amount of uncrystalline phases that are quite different from the cement made by Sugama and Carciello [3]. Fig. 2 shows the typical XRD patterns of sample no. 022 in region (a). Both CA and $\alpha\text{-}C_3P$ belong to monoclinic system (JCPDS cards 23-1036 and 9-348); the character d-spaces (by XRD) are 0.2963 and 0.2901 nm, respectively. Phase S belongs to cubic system, because the crystal grains present total extinction under the cross-polarization microscope. The main d-spaces of XRD patterns of phase S are: 0.6508, 0.3745, 0.3245, 0.2901, 0.2649,0.2451, 0.2291, 0.2160, 0.1871, 0.1798, 0.1620, and 0.1573 nm, which could not be matched by any present JCPDS cards. ESCA, shown in Fig. 3, suggests that the composition of some particles is very close to that of phase S synthesized by Zhang [8], so the quaternary compound presented here is believed to be phase S, with its possible chemical composition given by electron probe shown in Eq. (2):

$$CaO \cdot (Al_2O_3)_{0.6571} \cdot (SiO_2)_{0.2787} \cdot (P_2O_5)_{0.1182} \quad (2)$$

3.2. Characterization of phase structure for APC

Fig. 4 shows the XPS fitting curve for ion Ca_{2p} in compound S. The possible four chemical states of Ca^{2+} ion in the structure of phase S might be identified from the knowledge on crystallochemistry, the Ca_{2P} XPS of CaO, $CaCO_3$, CaF_2, and $CaTiO_3$ [9], and the definition of BE that 347.00 and 347.70 eV correspond to the states of coordination number (CN) 6 and 8, respectively; that 346.05 and 347.70 eV might correspond with the states of CN 5 and 9, respectively. It implies that the coordination state of ion Ca^{2+} is irregular in lattice structure, and that the opening structure would be created easily, which will cause compound S to have hydraulic behavior.

As to phases CA and $\alpha\text{-}C_3P$, samples no. 022 and no. 024 can be used as examples. Fig. 5 shows the IR spectra of these two samples compared to pure phases CA and $\alpha\text{-}C_3P$

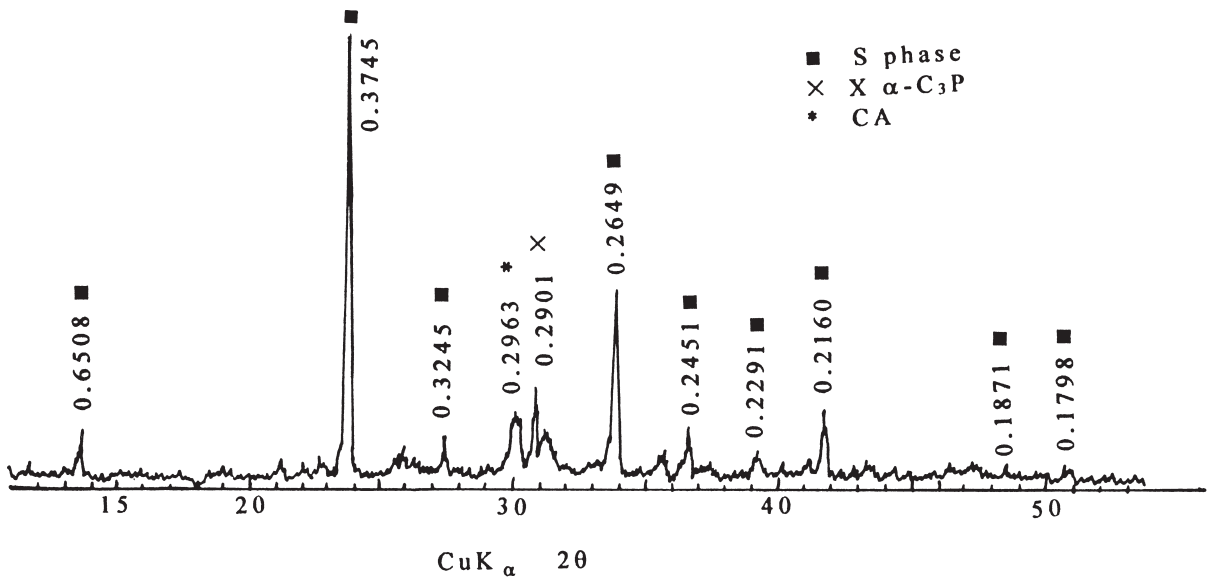

Fig. 2. Typical XRD patterns of sample no. 022 in region (a).

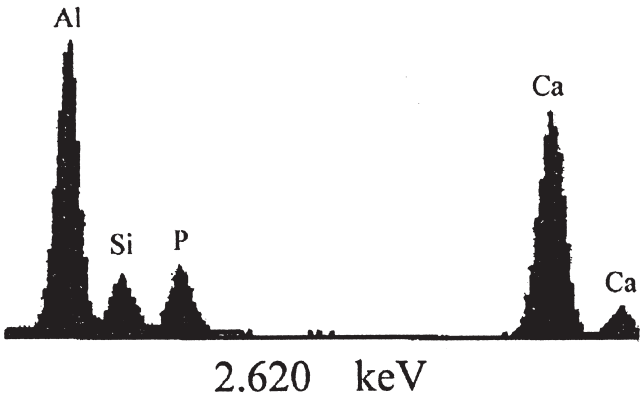

Fig. 3. Electron-dispersive X-ray analysis spectra of phase S.

synthesized by the authors through sol-gel routine and verified by XRD. It can obviously be seen that the absorption bands become broad and weak, especially at the range of 1062–1010 cm^{-1} for radical $\nu_{as}[PO_4]^{3-}$ and 870–760 cm^{-1}, 725–636 cm^{-1} for $\nu_{as}[AlO_4]^{5-}$ and $\nu_s[AlO_4]$, respectively [10]. Band 1107 cm^{-1} for sample no. 022 or 1103 cm^{-1} for sample no. 024 indicate that dimer of $[PO_4]$ group may have formed [11] and that the orderly degree of $[PO_4]$ group might have reduced by the mutual substitution of ions (P^{5+}, Al^{3+}, and Si^{4+}) and by the defect reactions mentioned above. XRD patterns in Fig. 2 show that phase CA with its main peak (d = 0.2963 nm) dividing is poorly crystallized here; the main patterns of phase α-C_3P, compared with JCPDS card 9-348, shifts from 0.2909 to 0.2901 nm (or to 0.289 nm for some other samples); and the background of patterns for both CA and α-C_3P is high. It might be inferred from the IR and XRD analyses that the modification of these two phases in APC could have taken place [12].

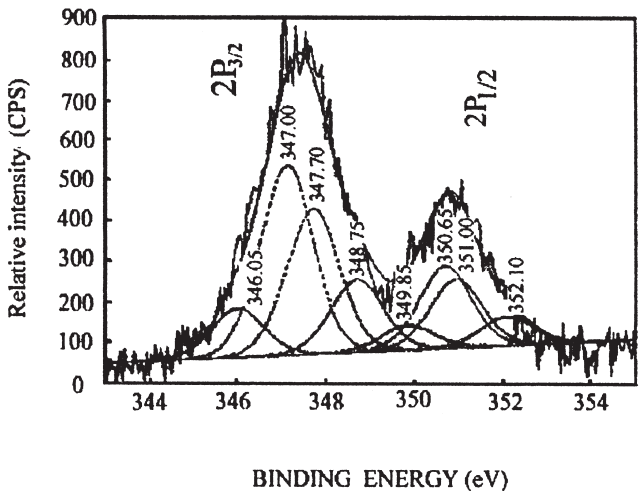

Fig. 4. Deconvolution curve of XPS for ion Ca_2P in compound S.

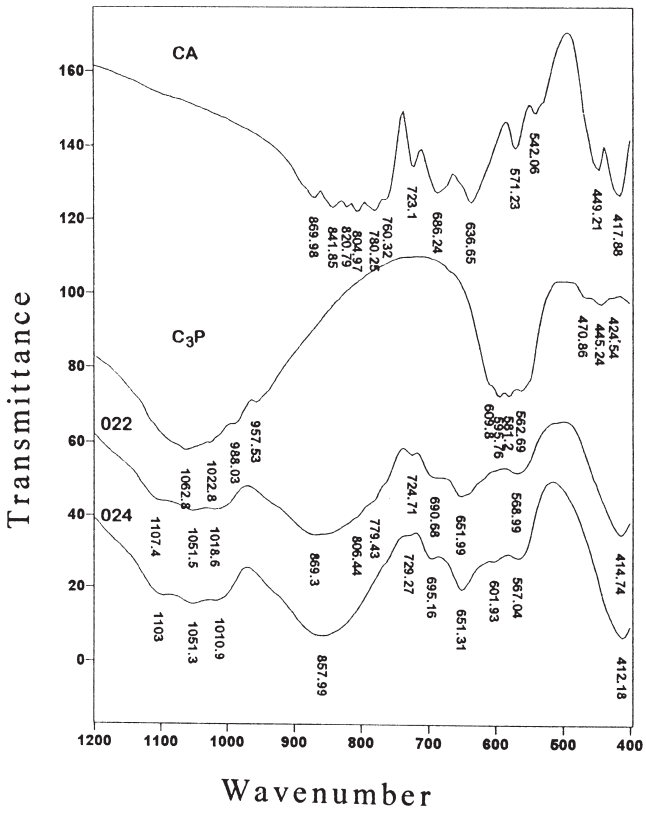

Fig. 5. IR spectra of samples no. 022 and no. 024 in region (a).

3.3. Compressive strength

In Fig. 1, region (b) should be regarded as noncementitious, because the compressive strength of pastes is too weak to be tested; region (a) should be regarded as cementitious. Fig. 6 shows that the compressive strength develops as the curing age increases for pastes with variable compositions in region (a). It can be seen that sample no. 022 exhibits early high and long-term high strength. The strength can go up to 152 MPa at 180 days, which is 33.33% higher than that at 28 days (114 MPa); the pastes of samples no. 023 and no. 024 exhibit fairly high strength in all the curing age, although the strength of sample no. 024 decreases slightly from 28 to 90 days. All of them possess a 1-day strength of 61–74 MPa. The early strength of samples no. 012, 013, and 021 is very low, but its rate of increase is high. Taking sample no. 13 as an example, the strength at 28 days is 28 times as high as that at 1 day, and it is 54% higher at 180 days than that at 28 days. It is interesting that there are four stages in the course of the strength development for sample no. 021 pastes. From 1 to 3 days and 28 to 90 days could be considered as an induction period, and from 3 to 28 days and 90 to 180 days as an acceleration period of strength increment.

However, why does the hydration behavior of samples in region (a) differ significantly from that in region (b)?

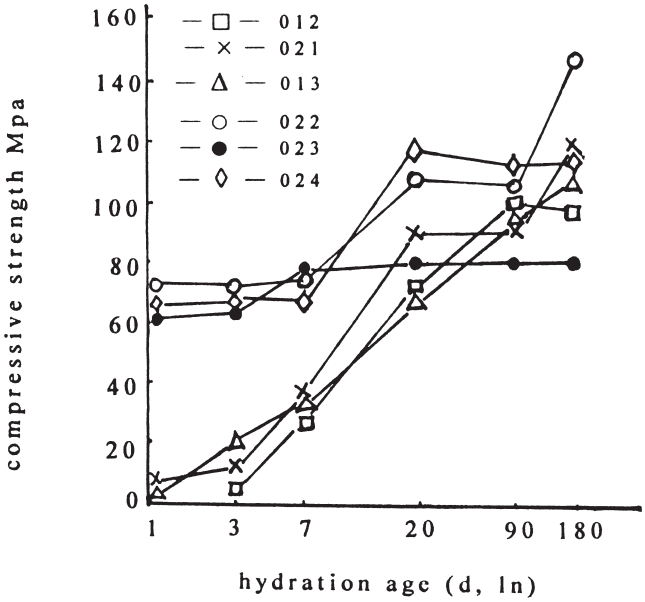

Fig. 6. Variation patterns of compressive strength with composition and the hydration age in hardening pastes.

3.4. Explanation on hydration performance in regions (a) and (b)

In Table 1, it can be seen first the basicity in region (a) is higher than that in region (b). This indicates that a necessary basicity in the paste is responsible for hydration and hardening. Second, along with the increasing molar ratio of $SiO_2/(Al_2O_3 + P_2O_5)$, the d-space of the main peak of phase S shifts lower from 0.3748 (in sample no. 024) to 0.3743 (in sample no. 12) and to 0.3734 (in sample no. 0.16), shown in Fig. 7. The structure of phase S might be fairly open, which allows additions to enter into its spaces easily. Meanwhile, the radius of the ion Si^{4+} is larger than that of P^{5+}(see Table 2); it is implied that the amount of Si^{4+} ion is responsible to a great extent for the hydration behavior of phase S, thereby for APC. Fig. 8 shows the IR spectra of samples no. 024, 012, and 016. These spectra have been published for the first time. With the basicity decreasing and the molar ratio of $SiO_2/(Al_2O_3 + P_2O_5)$ increasing (see Table 1), the absorption bands of $\nu_{as}[PO_4]$ at 1010.94 and 1051.52 cm^{-1} are gradually reducing the degeneration and become more and more sharp from samples no. 024 to 012 to 016, as does the band 858 cm^{-1}. The absorption band of $\nu_s[AlO_4]$ shifts higher from 651.3 cm^{-1} (sample no. 024) to 655.04 cm^{-1} (sample no. 012), and to 658.34 cm^{-1} (sample no. 016). This suggests that the symmetry of $[AlO_4]$ group is promoted, and that the bond energy is getting stronger and stronger. In connection with the above reasons, it explains why region (a) is cementitious but region (b) is not, although the main crystal phase S is present in it. In other words, an excessive amount of Si^{4+} will act as a stabilizer in the lattice structure. The substitution of ion Si^{4+} for Al^{3+} or P^{5+} is very limited for a good hydration behavior of phases for APC pastes.

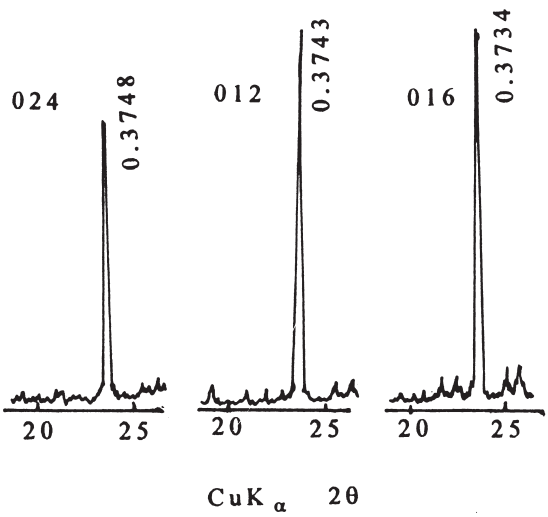

Fig. 7. XRD character pattern shifting of phase S for typical samples in the regions (a): samples no. 024, 012; and region (b): sample no. 016.

4. Conclusions

1. There are cementitious and noncementitious regions in the quaternary system $CA\text{-}C_{12}A_7\text{-}P_2O_5\text{-}SiO_2$.

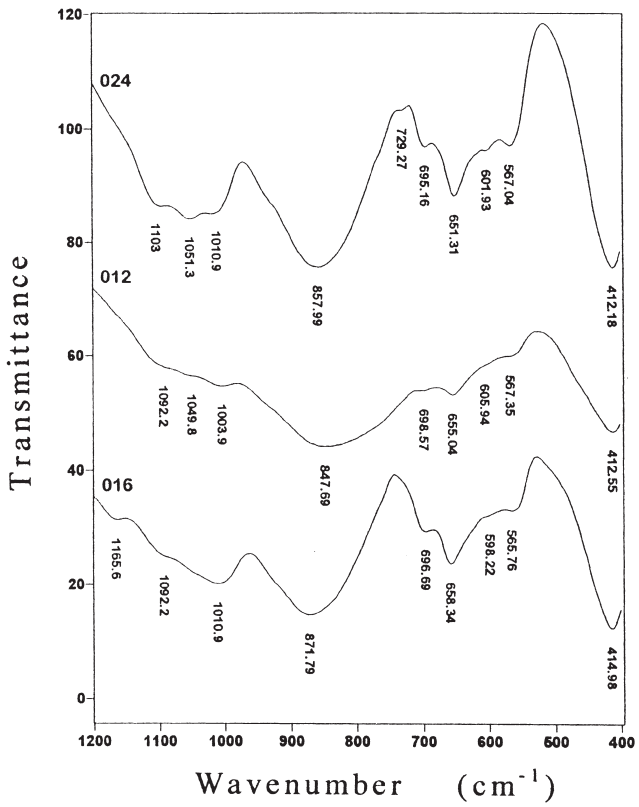

Fig. 8. IR spectra of samples in region (a): samples no. 024, 012; and region (b): sample no. 016.

2. The APC studied here has the performance of early high and increasing long-term strength, thanks to the new quaternary compound S, modified α-C_3P and CA, and a certain amount of amorphous phase.
3. Controlling the basicity and molar ratio of SiO_2/(Al_2O_3+P_2O_5) in APC is necessary to obtain high cementitious performance.

Acknowledgments

Authors would like to thank National Science Foundation of China (59472030) and Shandong Province Natural Science Foundation of China (Y94F1265) for the financial supporting of this research project.

References

[1] W.D. Kingery, Fundamental study of phosphate bonding in refractories I-III, J Am Ceram Soc 33 (8) (1995) 239–250.
[2] J.E. Cassidy, Phosphate bond then and now, Ceramic Bulletin 56 (7) (1977) 640–643.
[3] T. Sugama, N. Carciello, Hydrothermally synthesized aluminum phosphate cements, Advances in Cement Research 5 (17) (1993) 31–40.
[4] T. Sugama, N. Carciello, Sodium phosphate-derived calcium phosphate cements, Cem Concr Res 25 (1) (1995) 91–101.
[5] F. Yonghao, S. Shuzhe, Y. Nanru, Study on CBC materials in system phosphate-high aluminum cement, Proceedings of 7th symposium on cement chemistry and analysis techniques, Jinan, China, 1996, pp. 30–36 (in Chinese).
[6] L. Peiwen, Fundamental Theory on Inorganic Materials Science, Wuhan Industrial University Press, Wuhan, China, 1996, pp. 95, 320 (in Chinese).
[7] W. Dianfen, Application of X-Ray Photoelectron Spectroscopy in Research of Non-Metallic Materials, Wuhan University of Technology Press, Wuha, China, 1944, pp. 13–26, 123–125.
[8] Z. Guohui, The study on cementitious of alumina-rich region in quaternary system CaO-Al_2O_3-SiO_2-P_2O_5, Master degree thesis, Shandong Building Materials Institute, China, 1996.
[9] C.D. Wagner, W.M. Riggs, L.E. Davis, J.F. Moulder, G.E. Mullenberg, Handbook of X-Ray Photoelectron Spectroscopy, Perkin-Elmer Co. USA, 1979.
[10] W. Lu, The Infrared Spectroscopy of Minerals, Chongqing University Press, Chongqing, China, 1988, p. 66.
[11] V.C. Famer (Ed.), Y. Yupu (Trans.), The Infrared Spectra of Minerals, Science Press, Beijing, 1982, pp. 7, 311 (in Chinese).
[12] L. Shiqun, Z. Guohui, Z. Ning, L. Biao, C. Wei, H. Jiashan, Study on hydraulic activation of aluminum-rich area in CaO-Al_2O_3-P_2O_5 system, J of the Chinese Ceramic Society 26 (2) (1998) 142–148 (in Chinese).